LAWRENCE
LIVERMORE
NATIONAL
LABORATORY

LLNL-TR-770159

Model-Based Localizatiion in a Shallow Ocean Environment: A Sequential Bayesian/Optimization Approach

J. V. Candy

March 21, 2019

Disclaimer

This document was prepared as an account of work sponsored by an agency of the United States government. Neither the United States government nor Lawrence Livermore National Security, LLC, nor any of their employees makes any warranty, expressed or implied, or assumes any legal liability or responsibility for the accuracy, completeness, or usefulness of any information, apparatus, product, or process disclosed, or represents that its use would not infringe privately owned rights. Reference herein to any specific commercial product, process, or service by trade name, trademark, manufacturer, or otherwise does not necessarily constitute or imply its endorsement, recommendation, or favoring by the United States government or Lawrence Livermore National Security, LLC. The views and opinions of authors expressed herein do not necessarily state or reflect those of the United States government or Lawrence Livermore National Security, LLC, and shall not be used for advertising or product endorsement purposes.

This work performed under the auspices of the U.S. Department of Energy by Lawrence Livermore National Laboratory under Contract DE-AC52-07NA27344.

Model-Based Localization in a Shallow Ocean Environment: A Sequential Bayesian/Optimization Approach

J. V. Candy

The shallow ocean is a dynamically changing medium leading to nonstationary statistical behavior when subjected to temperature, wind, surface variations, bottom interactions, noise and extraneous disturbances as well as other conditions that render it a uniquely challenging environment — especially from a signal processing perspective. Processors must account for and adapt to such instantaneous changes in order to be effective. Thus, a processor is required to "adapt" to these environmental variations while simultaneously providing meaningful estimates that are necessary for such applications as detection, localization, inversion and enhancement. In this paper, we develop a parametrically adaptive, sequential Bayesian processor capable of jointly estimating both modal functions and environmental parameters to provide enhanced estimates for a focused optimizer capable locating a target in the noisy shallow ocean environment.

1 INTRODUCTION

The shallow ocean environment presents a formidable challenge to many processing problems ranging from the simple enhancement of noisy measurements to detection, localization, inversion and source tracking [1]-[4]. This ever-changing, uncertain medium is caused by a variety of both inherent effects such as temperature variations altering the sound-speed profile leading to a highly dispersive medium inhibiting sound propagation. Corresponding to this fundamental effect are surface effects caused by the wind leading to undesirable wave motion routinely present. Internal disturbances abound created by a wealth of random biologics including high-frequency snapping shrimp to whale soundings as well as ambient noise from distant shipping in heavily occupied transportation channels [1]. Coupling this with the usual instrumentation noise and uncertainty creates a difficult acoustic problem to unravel especially for that of locating a quiet target hiding in a shallow ocean channel. All in all, the shallow ocean presents, perhaps one of the most challenging environments to extract meaningful information from noisy acoustic measurements. With all of these uncertainties and instantaneous changes, statistically, the underlying problem is clearly nonstationary requiring a sequential approach capable of incorporating these complex interactions along with the inherent variations and uncertainties that evolve.

One suite of methods that attack this complexity problem is model-based, that is, the incorporation of ocean acoustic models into the processing scheme [5]. Model-based techniques offer high expectations of performance, since the processor incorporates phenomenological information that has generated the measured data. But model inaccuracies can lead directly

to erroneous results, especially if the varying spatial/temporal nature of this environment is not taken into account. Therefore, all of these constraints require a sequentially adaptive processing scheme that must be able too cope with and extract both the signals of interest as well as their embedded parameters. Adaptive processing for the varying shallow ocean environment can be accomplished in a number of different ways. Here we concentrate on the "parametrically adaptive" approach, that is, a processor that embeds an ocean acoustic model into its framework and sequentially estimates both the modal functions as well as their embedded physical parameters [6], [7]. Thus, the processor must solve a joint modal enhancement and parameter estimation problem. As a solution to this problem, we develop a Bayesian processor capable of providing a joint solution to the modal function tracking and environmental adaptivity problem. The posterior distribution required is multi-modal (multiple peaks) requiring a sequential approach. Bayesian sequential processing that incorporates both a propagation model along with its inherent parameters offers a robust, parametrically adaptive solution that can cope with this instantaneously varying medium. Sequential Bayesian techniques enable a class of processors capable of performing in an uncertain, nonstationary, non-Gaussian, instantaneously changing, shallow ocean environment [7].

We select the normal-mode (shallow ocean) propagation model with inherent modal functions and pressure-field measurements as the signals of interest along with a set of modal coefficients as the parameters to be jointly estimated [7]. Here we concentrate on the parametrically adaptive approach, that is, a processor that incorporates an ocean acoustic model into its framework and sequentially estimates both the signals of interest as well as its embedded physical parameters. Bayesian sequential processing incorporating propagation models along with their inherent environmental parameters as well as measurement and noise models offers a robust, parametrically adaptive solution to signal processing problems in such a nonstationary environment [3]. Sequential Bayesian techniques enable a class of processors capable of performing in an uncertain, nonstationary (varying statistics), non-Gaussian, variable shallow ocean environment. Here we address the problem of estimating or tracking modal functions in a noisy shallow ocean while jointly adjusting (adaptively) the inherent propagation model parameters [3], [6], [7]. Using this information, we address the problem of localizing the position of an acoustic target from noisy hydrophone measurements gathered from a vertical sensor array. By simultaneously enhancing the measured pressure-field and estimating the corresponding modal functions, we can provide parametric (modal coefficients) estimates to a focused localizer. The localizer then enables an implicit position solution using a nonlinear cost function, while jointly adjusting (adaptively) the inherent propagation model parameters. In this manner, the combined model-based processing/optimization technique is able to extract the target range and depth location. Initially, incorporating a propagation model into a signal processing scheme to solve the source localization problem was initiated by matching a modal function of an acoustic waveguide to estimate source depth [8], [9]. The concept of matched-field processing (MFP), that is, comparing the measured pressure-field to that predicted by a propagation model was introduced

[8] and applied to a variety of problems. It provided a solution to the localization problem by repeated model predictions at the array for various assumed source positions enabling a search for not only the target of interest but also all other possible acoustic sources in the search region. Derivative techniques have evolved by matching modal functions demonstrating an improvement in performance [8]-[17]. Many papers have been written exploiting and improving on the MFP [8]. Other statistical approaches to solve the localization problem have also evolved again illustrating well-founded enhanced performance [19]-[22]. However, in this paper, we investigate the state-space forward propagation scheme of Refr. [6] and apply it to this problem.

The fundamental concept introduced in this work remains intact; however, with the embedded processor (extended Kalman filter) replaced by a sequential Bayesian processor—the particle filter to provide enhanced estimates to the focused localizer. In contrast to other popular approaches in which the acoustic propagation model is just employed in the measurement model, this model-based localization method integrates the normal-mode solutions into both the state (forward propagator) and measurement (pressure-field) relations [6]. Here the particle filter is the parametrically adaptive processor incorporating both an ocean acoustic normal-mode model as well as the pressure-field measurement obtained from a vertical sensor array deployed in the sound channel [7]. Thus we see that it is, in fact, the parametrically adaptive processor that provides the heart of the model-based localization scheme. This technique, as before in Refr. [6], is better thought of as a means to "focus" on a target of interest, when the entire search region has already been specified. This approach incorporates the particle filter as the primary method to provide the enhanced pressure-field measurements as part of the joint estimation solution required to jointly extract the modal functions estimates and extract the accompanying modal coefficients provided to the optimizer for target localization.

In this manner, the combined model-based processing/optimization technique is able to extract the target range and depth location. A simple diagram of this approach is shown in Fig. 1 where we observe the raw pressure-field input from a vertical hydrophone sensor array along with the sound-speed data available from current-temperature-density (CTD) sensors or historical archive data. With the input data available, the parametrically adaptive processor uses the embedded normal-mode, forward propagator, pressure-field measurement and noise models to extract estimates of the modal functions and corresponding coefficients. With these enhanced estimates now available on input, the coupled optimizer provides estimates of the source position information (range/depth).

We first characterize the normal-mode model in terms of a state-space representation enabling a general framework for signal processing in Sec. 2 leading to the formulation of the forward propagators. We also develop the parametrically adaptive processor by augmenting a random walk model of the modal coefficients into the normal-mode representation. In Sec. 3, we formulate the sequential Bayesian processor construct leading to the corresponding "bootstrap" particle filter design for our application. In Sec. 4, the optimization scheme is presented employing, as before [6], the Nelder-Meade simplex technique. Finally, we discuss

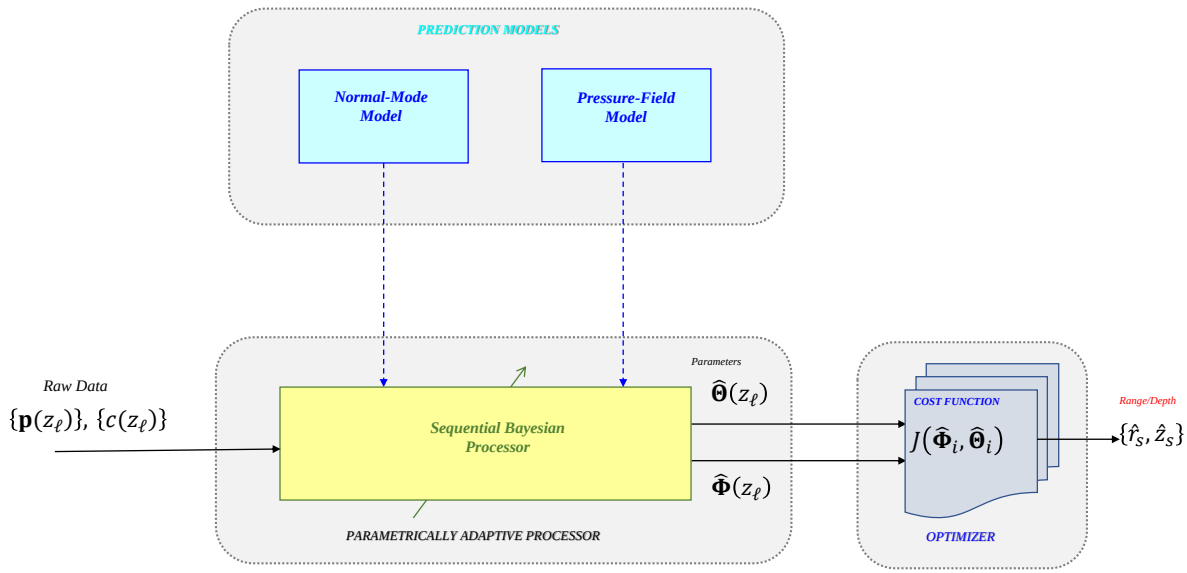

Figure 1: Model-Based Localization: the Basic Processor consisting of prediction models (modes and pressure-field), parametrically adaptive processor and optimizer.

the application of this approach to data from the well-known Hudson Canyon experiment [23], [24] in Sec. 5 and then summarize our results.

2 BACKGROUND

In this section we provide a brief discussion of the underlying models employed to develop the parametrically adaptive approach for source localization. We start with the normal-mode and pressure-field ocean acoustic models and discuss how they are incorporated into a state-space framework enabling the development of the subsequent processor followed by the corresponding Gauss-Markov model and the representation utilized in the parametrically adaptive processor to follow.

2.1 Shallow Ocean Model

Assuming a horizontally-stratified ocean of depth h with a *known* horizontal source range r_s and depth z_s and the assumption that the acoustic energy from a point source can be modeled as a trapped wave governed by the Helmholtz equation evolves [1]. Removing the time dependence and performing the standard separation of variables technique and leads to a set of ordinary differential equations, that is, we obtain a "depth only" representation of the wave equation which is an eigenvalue equation in z with

$$\frac{d^2}{dz^2}\phi_m(z) + \kappa_z^2(m)\phi_m(z) = 0, \; m = 1, \cdots, M, \tag{1}$$

whose eigensolutions $\{\phi_m(z)\}$ are the *modal functions* and κ_z is the vertical wavenumber in the z-direction. These solutions depend on the sound speed profile $c(z)$ and the boundary conditions at the surface and bottom as well as the corresponding *dispersion* relation given by

$$\kappa^2 = \frac{\omega^2}{c^2(z)} = \kappa_r^2(m) + \kappa_z^2(m), \qquad m = 1, \ldots, M, \tag{2}$$

where $\kappa_r(m)$ is the horizontal wavenumber associated with the m-th mode in the r direction and ω is the harmonic source frequency.

By assuming a known horizontal source range *a priori*, we obtain a range solution given by the Hankel function, $H_0(\kappa_r r_s)$ enabling the pressure-field to be represented by

$$p(r_s, z_s, z) = \sum_{m=1}^{M} \theta_m(r_s, z_s)\phi_m(z), \tag{3}$$

where p is the acoustic pressure; ϕ_m is the mth modal function with the modal coefficient defined by

$$\theta_m(r_s, z_s) := q\ H_0(\kappa_r r_s)\ \phi_m(z_s), \tag{4}$$

a function of source location (r_s, z_s) with q the source amplitude scaling factor.

2.2 State-space Ocean Acoustic model

The depth-only eigen-equation can easily be transformed to state-space form by defining the state vector of the m-th mode as

$$\phi_m(z) := \begin{bmatrix} \phi_m(z) \\ \frac{d}{dz}\phi_m(z) \end{bmatrix} = \begin{bmatrix} \phi_{m1}(z) \\ \phi_{m2}(z) \end{bmatrix}. \tag{5}$$

Thus, we have for the m-th mode the following state (vector) equation as:

$$\frac{d}{dz}\phi_m(z) = \mathbf{A}_m(z)\phi_m(z), \tag{6}$$

for

$$\mathbf{A}_m(z) = \begin{bmatrix} 0 & 1 \\ -\kappa_z^2(m) & 0 \end{bmatrix}. \tag{7}$$

Assuming that the ocean acoustic noise can be characterized by additive uncertainties, we can extend the deterministic state equation for the M-modes, that is, $\Phi(z) := [\phi_1(z)|\cdots|\phi_M(z)]'$ leading to the following $2M$-dimensional Gauss-Markov representation of the model:

$$\frac{d}{dz}\phi(z) = \mathbf{A}(z)\phi(z) + \mathbf{w}(z), \tag{8}$$

where $\mathbf{w}(z) = [w_1 \quad w_2 \quad \ldots \quad w_{2M}]'$ is additive, zero-mean, Gaussian random noise. The system matrix $\mathbf{A}(z)$ is defined as

$$\mathbf{A}(z) = \begin{bmatrix} \mathbf{A}_1(z) & \cdots & 0 \\ \vdots & \ddots & \vdots \\ 0 & \cdots & \mathbf{A}_M(z) \end{bmatrix}, \tag{9}$$

with the overall state vector is

$$\phi(z) = [\phi_{11} \quad \phi_{12} \mid \phi_{21} \quad \phi_{22} \mid \quad \ldots \quad \mid \phi_{M1} \quad \phi_{M2}]'. \tag{10}$$

This leads to a set of *measurement* equations that can expressed as

$$p(r_s, z_s, z) = \mathbf{C}'(r_s, z_s)\phi(z) + v(z), \tag{11}$$

where

$$\mathbf{C}'(r_s, z_s) = [\theta_1(r_s, z_s) \;\; 0 \mid \;\; \cdots \;\; \mid \theta_M(r_s, z_s) \;\; 0]\,. \tag{12}$$

The random noise terms $\mathbf{w}(z)$ and $v(z)$ are assumed Gaussian and zero-mean with respective covariance matrices, $\mathbf{R}_{ww}$ and $\mathbf{R}_{vv}$. The measurement noise ($v(z)$) is used to represent the "lumped" effects of near-field acoustic noise field, flow noise on the hydrophone and electronic noise. The modal noise ($\mathbf{w}$) can be used to represent the "lumped" uncertainty of sound speed errors, distant shipping noise, errors in the boundary conditions, sea state effects and ocean inhomogeneities that propagate through the ocean acoustic system dynamics (normal-mode model). These assumptions, with known model parameters lead to the optimal solution of the state estimation problem (Kalman filter) [25].

Since a vertical array spatially samples the pressure-field discretizing depth, we choose to discretize the state differential equations using a central difference approach for improved numerical stability, that is, from Eq. 1 we have

$$\frac{d^2}{dz^2}\phi_m \approx \frac{\phi_m(z_\ell) - 2\phi_m(z_{\ell-1}) + \phi_m(z_{\ell-2})}{\triangle z_\ell^2}, \tag{13}$$

for $\triangle z_\ell := z_\ell - z_{\ell-1}$.

Applying this approximation to Eq. 1 gives

$$\phi_m(z_\ell) - 2\phi_m(z_{\ell-1}) + \phi_m(z_{\ell-2}) + \triangle z_\ell^2 \kappa_z^2(m)\phi_m(z_{\ell-1}) = 0,$$

where z_ℓ is the location of the ℓ-th sensor. Defining the discrete modal state vector as $\phi_m(z_\ell) := [\phi_m(z_{\ell-2}) \mid \phi_m(z_{\ell-1})]'$, we obtain the following set of difference equations for the m-th mode as

$$\begin{aligned} \phi_{m1}(z_\ell) &= \phi_{m2}(z_{\ell-1}) \\ \phi_{m2}(z_\ell) &= -\phi_{m1}(z_{\ell-1}) + (2 - \triangle z_\ell^2 \kappa_z^2(m))\phi_{m2}(z_{\ell-1}), \end{aligned} \tag{14}$$

with each of the corresponding modal submatrices given by

$$A_m(z_\ell) = \begin{bmatrix} 0 & 1 \\ -1 & 2 - \triangle z_\ell^2 \kappa_z^2(m) \end{bmatrix}; \quad m = 1, \cdots, M, \tag{15}$$

and dispersion relation

$$\kappa_z^2(m) = \left(\frac{\omega^2}{c^2(z)}\right) - \kappa_r^2(m), \quad m = 1, \cdots, M. \tag{16}$$

Substituting this model and combining *all* of the modes as in Eq. 8, the following complete discrete *Gauss-Markov* representation of the normal-mode process and measurement system is

$$\begin{aligned} \mathbf{\Phi}(z_\ell) &= \mathbf{A}(z_\ell)\mathbf{\Phi}(z_{\ell-1}) + \mathbf{w}(z_\ell), \\ p(r_s, z_\ell) &= C'(r_s, z_s)\mathbf{\Phi}(z_\ell) + v(z_\ell), \end{aligned} \tag{17}$$

and $\mathbf{\Phi}, \mathbf{w} \in \mathcal{R}^{2M\times 1}$, $p, v \in \mathcal{R}^{1\times 1}$ for $\mathbf{w} \sim \mathcal{N}(0, R_{ww})$, $v \sim \mathcal{N}(0, R_{vv})$ and $\mathbf{\Phi}(z_\ell) \sim \mathcal{N}(\overline{\mathbf{\Phi}}(z_0), \overline{P}(z_0))$ and $\mathbf{A} \in \mathcal{R}^{2M\times 2M}$, a block diagonal matrix defined by $\mathbf{A}(z_\ell) := \text{diag}[A_1(z_\ell) \cdots A_M(z_\ell)]$, $C' \in \mathcal{R}^{1\times 2M}$ for M-modes and L-hydrophone sensors.

This completes the normal-mode/pressure-field representation of the shallow ocean in state-space form. Next we consider augmenting incorporating the set of unknown modal coefficients to create the parametrically adaptive processor.

2.3 Parametrically Adaptive State-space Model

A "parametrically adaptive" processor evolves from the normal-mode/pressure-field representation by defining a parameter set of interest. Variations in the ocean can be represented, parametrically, in a number of ways. For instance, modal variations can be reflected through the measured pressure-field relations of Eq. 3 that can be parametrically captured by the modal coefficients of Eq. 4. We note that these coefficients are a function of the source location (r_s, z_s) making this parameter set desirable for location solutions. Therefore, we choose to use the modal coefficients (individually) as the parameters of interest in adapting to the changing shallow ocean environment especially since they depend on the unknown source position [6].

The modal coefficients of Eq. 4 can be used to capture modal function variations; therefore, we define the set of unknown *modal parameters* for this problem as $\{\theta_m(r_s, z_s)\}$; $m = 1, \cdots, M$. and the new "augmented" state vector for the m-th mode incorporating the modal coefficients as

$$\Phi_m(z_\ell; \theta_m) := \Phi_m(z_\ell) = [\phi_{m1}(z_\ell)\ \phi_{m2}(z_\ell) \mid \theta_m(z_\ell)]'.$$

With this choice of parameters (modal coefficients) the augmented state equations for the m-th mode become

$$\begin{aligned} \phi_{m1}(z_\ell) &= \phi_{m2}(z_{\ell-1}) + w_{m1}(z_{\ell-1}) && \text{[Modal Functions]} \\ \phi_{m2}(z_\ell) &= -\phi_{m1}(z_{\ell-1}) + (2 - \triangle z_\ell^2 \kappa_z^2(m))\phi_{m2}(z_{\ell-1}) + w_{m2}(z_{\ell-1}) \\ \theta_m(z_\ell) &= \theta_m(z_{\ell-1}) + w_{\theta_m}(z_{\ell-1}) && \text{[Modal Coefficients]}, \end{aligned} \tag{18}$$

where we have modeled the unknown modal coefficients as a *random walk* ($\dot{\theta}_m(z) = w_{\theta_m}(z)$) to capture the variations of the modal coefficients with additive, zero-mean, Gaussian noise of covariance $R_{w_{\theta_m} w_{\theta_m}}$.

Here the random walk model provides "soft" constraints in the simulation, since the parameters are modeled as Gauss-Markov implying that 95% of the samples must lie within confidence limits controlled by ($\pm 1.96\sigma_{m,m}$). This constitutes a *soft* statistical constraint of the parameter variations. For our problem, we use the implied soft statistical constraint and choose to start the processor with initial parameter estimates close to those values other researchers have meticulously estimated from this data set [25]. More succinctly for the m-th mode, we can write

$$\Phi_m(z_\ell) = A_m(z_{\ell-1};\theta)\Phi_m(z_{\ell-1}) + \mathbf{w}_m(z_{\ell-1}) \tag{19}$$

or expanding

$$\underbrace{\begin{bmatrix} \phi_m(z_\ell) \\ --- \\ \theta_m(z_\ell) \end{bmatrix}}_{\Phi_m(z_\ell)} = \underbrace{\begin{bmatrix} A_m(z_{\ell-1}) & | & 0 \\ -- & & -- \\ 0 & | & 1 \end{bmatrix}}_{A_m(z_{\ell-1};\theta)} \underbrace{\begin{bmatrix} \phi_m(z_{\ell-1}) \\ --- \\ \theta_m(z_{\ell-1}) \end{bmatrix}}_{\Phi_m(z_{\ell-1})} + \underbrace{\begin{bmatrix} W_{\phi_m}(z_{\ell-1}) \\ --- \\ W_{\theta_m}(z_{\ell-1}) \end{bmatrix}}_{\mathbf{w}_m(z_{\ell-1})}, \tag{20}$$

where $W_{\phi_m} \sim \mathcal{N}(0, R_{W_{\phi_m} W_{\phi_m}})$, $W_{\theta_m} \sim \mathcal{N}(0, R_{W_{\theta_m} W_{\theta_m}})$, $\phi_m(0) \sim \mathcal{N}(\overline{\phi}_m(0), R_{\phi_m \phi_m})$, $\theta_m(0) \sim \mathcal{N}(\overline{\theta}_m(0), R_{\theta_m \theta_m})$, and

$$A_m(z_{\ell-1};\theta) = \begin{bmatrix} 0 & 1 & | & 0 \\ -1 & 2 - \triangle z_{\ell-1}^2 \kappa_z^2(m) & | & 0 \\ - & - & - & \\ 0 & 0 & | & 1 \end{bmatrix}$$

with A a block diagonal matrix such that $A(z_{\ell-1};\theta) = \mathrm{diag}[A_1(z_{\ell-1};\theta), \cdots, A_M(z_{\ell-1};\theta)]$.

The corresponding nonlinear measurement model is given by

$$p(r_s, z_s, z_\ell) = \sum_{m=1}^{M} \theta_m(z_\ell)\phi_m(z_\ell) + v(z_\ell);\ \ell = 1, \cdots, L, \tag{21}$$

with dispersion (sound-speed)

$$c(z_\ell) = \frac{\omega}{\sqrt{\kappa_z^2(m) + \kappa_r^2(m)}},\ m = 1, \cdots, M;\ \ell = 1, \cdots, L \tag{22}$$

To complete this representation, we combine all of the modes and unknown parameters and therefore the state transition is characterized by the underlying augmented state-space model as

$$\mathbf{\Phi}(z_\ell;\Theta) = \mathbf{A}(z_{\ell-1};\Theta)\mathbf{\Phi}(z_{\ell-1};\Theta) + \mathbf{w}(z_{\ell-1}),$$

and the measurement, on the other hand, is determined from the nonlinear pressure-field measurement model,

$$p(r_s, z_s, z_\ell) = \mathbf{c}\Big[\mathbf{\Phi}(z_\ell);\Theta(r_s, z_s)\Big] + v(z_\ell). \tag{23}$$

Note that the pressure-field is nonlinear in the states (modal functions) and parameters (modal coefficients), since they are multiplicands and therefore lead to non-Gaussian measurements.

It should also be noted that the *initial* model parameters are obtained from a prior solution of the boundary value problem typically developed as part of the experimental design process and/or after the experiment has been executed. Here the initial "guesses" at modal coefficients and modal functions themselves are calculated based on the experimental conditions such as frequencies, current-temperature-density (*CTD*), archival sound-speed profiles (*SSP*), boundary conditions, horizontal wavenumber estimators (e.g. see [23], [24] for more details) to provide the input to the normal-mode boundary-value problem (*BVP*) solutions (SNAP [26], [27], KRACKEN [28], SAFARI [29]) yielding the required parameters. These parameters are then input to the state-space, measurement, and noise/uncertainty models as shown in Fig. 2.

This completes the section on the discrete state-space representation of the shallow ocean acoustic (normal-mode) propagation model that is embedded as a "forward propagator" into the subsequent processors for signal enhancement.

3 SEQUENTIAL BAYESIAN PROCESSOR

In this section we discuss the processor for the shallow oceanic problem [1], [27]. The basic adaptive problem can be defined in terms of our mathematical models as:

GIVEN, $[\{p(r_s, z_s, z_\ell)\}, \{c(z_\ell)\}]$, a set of noisy pressure-field and sound speed measurements varying in depth along with the underlying state-space model of Eqs. 19, 21 and 22 with unknown parameters $\{\theta(z_\ell)\}$, FIND the "best" (minimum error variance) estimates (joint) of the modal functions and parameters, that is, $\{\hat{\phi}_m(z_\ell)\}, \{\hat{\theta}_m(z_\ell)\}; m = 1, \cdots, M$ and measurements $\{\hat{p}(r_s, z_s, z_\ell)\}$.

The solution to this problem lies in the *joint state/parameter estimation* problem, that is, defining the *augmented state vector*,

$$\mathbf{\Phi}(z_\ell;\mathbf{\Theta}) := \begin{bmatrix} \mathbf{\Phi}(z_\ell) \\ --- \\ \mathbf{\Theta}(z_\ell) \end{bmatrix},$$

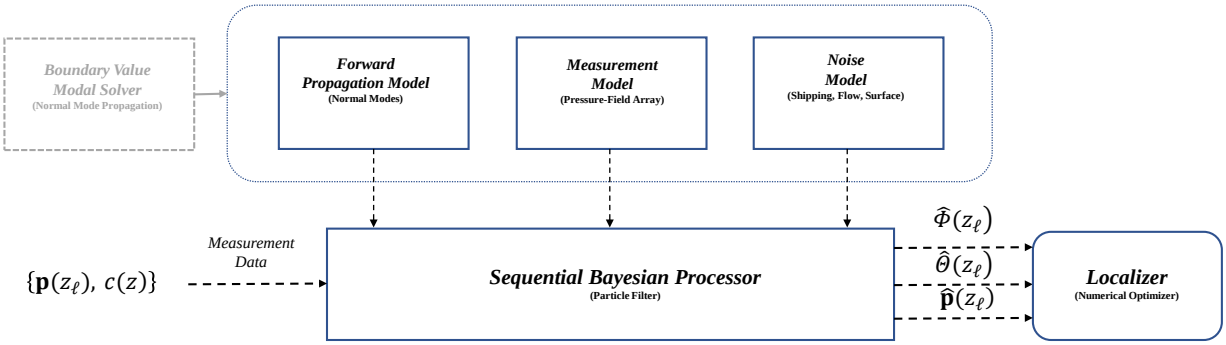

Figure 2: Model-based processor design: (a) Boundary solver for initial parameters. (b) Propagator, measurement and noise/uncertainty models. (c) *MBP*. (d) Applications: localization, enhancement (tracking) and inversion.

and starting with the joint distribution applying Bayes' theorem, we obtain [30]

$$\Pr[\mathbf{\Phi}(z_\ell;\mathbf{\Theta})|P_\ell] = \left(\frac{\Pr\Big[p(r_s,z_s,z_\ell)|\mathbf{\Phi}(z_\ell;\mathbf{\Theta})\Big] \times \Pr\Big[\mathbf{\Phi}(z_\ell;\mathbf{\Theta})|\mathbf{\Phi}(z_{\ell-1};\mathbf{\Theta})\Big]}{\Pr\Big[p(r_s,z_s,z_\ell)|P_{\ell-1}\Big]}\right) \times \Pr[\mathbf{\Phi}(z_{\ell-1};\mathbf{\Theta})|P_{\ell-1}], \tag{24}$$

where we have assumed conditional independence and defined the set of measurements as $P_\ell := \{p(r_s,z_s,z_1),\cdots,p(r_s,z_s,z_\ell)\}$.

Define the *joint weighting function* in terms of the likelihood, transition and evidence as

$$W(z_\ell;\mathbf{\Theta}) := \left(\frac{\Pr\Big[p(r_s,z_s,z_\ell)|\mathbf{\Phi}(z_\ell;\mathbf{\Theta})\Big] \times \Pr\Big[\mathbf{\Phi}(z_\ell;\mathbf{\Theta})|\mathbf{\Phi}(z_{\ell-1};\mathbf{\Theta})\Big]}{\Pr\Big[p(r_s,z_s,z_\ell)|P_{\ell-1}\Big]}\right), \tag{25}$$

yielding the *sequential* Bayesian posterior distribution as

$$\Pr[\mathbf{\Phi}(z_\ell;\mathbf{\Theta})|P_\ell] = W(z_\ell;\mathbf{\Theta}) \times \Pr[\mathbf{\Phi}(z_{\ell-1};\mathbf{\Theta})|P_{\ell-1}]. \tag{26}$$

The processor for the non-Gaussian problem is the particle filter. It is a completely different approach to nonlinear filtering in that it removes the restriction of additive Gaussian noise sources and is clearly capable of characterizing multi-modal distributions. The *PF* can be thought of as a histogram or kernel density-like estimator in the sense that it generates an empirical probability mass function (*PMF*) that approximates the desired *posterior distribution* such that statistical inferences can be performed and statistics extracted directly. Here the idea is to develop an empirical estimation of the posterior distribution following a purely Bayesian approach using Monte Carlo (*MC*) sampling theory as its enabling foundation. The computational burden of the *PF* is much higher that of *KF*, since it must provide an estimate of the underlying state posterior distribution component-by-component at *each* z_ℓ-step and the number of samples to characterize the posterior distribution is equal to the number of particles.

Here we are concerned with the joint estimation problem consisting of setting a prior for θ and augmenting the state vector to solve the joint estimation problem as defined above thereby converting the parameter estimation problem to one of optimal filtering. Thus, the particle filter estimates the weights required to specify the posterior distribution, empirically, that is,

$$\hat{\Pr}[\mathbf{\Phi}(z_\ell;\mathbf{\Theta})|P_\ell] \approx \frac{1}{N_p}\sum_{i=1}^{N_p}\hat{\mathcal{W}}_i(z_\ell;\mathbf{\Theta}) \times \delta\left(\mathbf{\Phi}(z_\ell;\mathbf{\Theta}) - \mathbf{\Phi}_i(z_\ell;\mathbf{\Theta})\right). \tag{27}$$

The approach is to estimate these weights based on the concept of importance sampling [30]-[33]. *Importance sampling* is a technique to compute statistics with respect to one distribution using random samples drawn from another. It is a method of simulating samples

from a proposal or sampling (importance) distribution to be used to approximate a targeted distribution (joint posterior) by appropriate weighting. For this choice, the weighting function is defined by

$$\mathcal{W}(z_\ell;\mathbf{\Theta}) := \frac{\Pr[\mathbf{\Phi}(z_\ell;\mathbf{\Theta})|P_\ell]}{\mathcal{I}[\mathbf{\Phi}(z_\ell;\mathbf{\Theta})|P_\ell]}, \tag{28}$$

where $\mathcal{I}[\cdot]$ is the proposed sampling or *importance distribution*.

For the "sequential" case, we have that the weighting function becomes [30]

$$\mathcal{W}(z_\ell;\mathbf{\Theta}) \propto \left(\frac{\Pr\Big[p(r_s,z_s,z_\ell)|\mathbf{\Phi}(z_\ell;\mathbf{\Theta})\Big] \times \Pr\Big[\mathbf{\Phi}(z_\ell;\mathbf{\Theta})|\mathbf{\Phi}(z_{\ell-1};\mathbf{\Theta})\Big]}{\mathcal{I}[\mathbf{\Phi}(z_\ell;\mathbf{\Theta})|\mathbf{\Phi}(z_{\ell-1};\mathbf{\Theta}),P_\ell]}\right) \times \mathcal{W}(z_{\ell-1};\mathbf{\Theta}), \tag{29}$$

where $\propto$ means *proportional to* up to a normalizing constant (evidence).

There are a variety of *PF* algorithms available, each evolving by a particular choice of the sampling or importance distribution, but perhaps the simplest is the *bootstrap* technique which we apply to our problem. Here the importance distribution is selected as the transition prior, that is,

$$\mathcal{I}\Big[\mathbf{\Phi}(z_\ell;\mathbf{\Theta})|\mathbf{\Phi}(z_{\ell-1};\mathbf{\Theta}),P_\ell)\Big] \longrightarrow \Pr\Big[\mathbf{\Phi}(z_\ell;\mathbf{\Theta})|\mathbf{\Phi}(z_{\ell-1};\mathbf{\Theta})\Big]. \tag{30}$$

Substituting into Eq. 29 we obtain

$$\mathcal{W}(z_\ell;\mathbf{\Theta}) = \Pr\Big[p(r_s,z_s,z_\ell)|\mathbf{\Phi}(z_\ell;\mathbf{\Theta})\Big] \times \mathcal{W}(z_{\ell-1};\mathbf{\Theta}). \tag{31}$$

Thus, we see that once the underlying posterior is available, the estimates of important statistics can be inferred directly. For instance, the maximum a posteriori (*MAP*) estimate is simply found by locating a particular particle $\hat{\phi}_i(z_\ell)$ corresponding to the maximum of the *PMF*, that is,

$$\hat{\mathbf{\Phi}}_i(z_\ell;\mathbf{\Theta})_{MAP} = \max_i \ \hat{\Pr}[\mathbf{\Phi}_i(z_\ell;\mathbf{\Theta})|P_\ell], \tag{32}$$

while the conditional mean or equivalently the minimum mean-squared error or the conditional mean (*CM*) estimate is calculated by integrating the posterior as:

$$\hat{\mathbf{\Phi}}_i(z_\ell;\mathbf{\Theta})_{CM} = \int \mathbf{\Phi}_i(z_\ell;\mathbf{\Theta}) \times \hat{\Pr}[\mathbf{\Phi}_i(z_\ell;\mathbf{\Theta})|P_\ell]dz \approx \frac{1}{N_p}\sum_{i=1}^{N_p} \mathcal{W}_i(z_\ell;\mathbf{\Theta}) \times \mathbf{\Phi}_i(z_\ell;\mathbf{\Theta}), \tag{33}$$

and N_p is the number of particles.

For the bootstrap implementation, we need only draw noise samples from the state and parameter distributions and use the dynamic models above (normal-mode/random

walk) in Eq. 19 to generate the set of particles, $\{\mathbf{\Phi}_i(z_\ell;\mathbf{\Theta})\} \longrightarrow \{\mathbf{\Phi}_i(z_\ell),\mathbf{\Theta}_i(z_\ell)\}$ for $i = 1,\cdots,N_p$. That is, both sets of particles are generated from the augmented models (linear/nonlinear)(adaptive modal coefficients) from

$$\mathbf{\Phi}_i(z_\ell;\Theta) = \mathbf{A}(z_{\ell-1})\mathbf{\Phi}_i(z_{\ell-1}) + \mathbf{w}_i(z_{\ell-1}) \tag{34}$$

while the likelihood is determined from the nonlinear pressure-field measurement model

$$p(r_s, z_s, z_\ell) = c\Big[\mathbf{\Phi}_i(z_\ell;\Theta)\Big] + v(z_\ell). \tag{35}$$

Assuming additive Gaussian noise the likelihood is given by

$$\Pr[p(r_s, z_s, z_\ell)|\mathbf{\Phi}_i(z_\ell)] = \frac{1}{\sqrt{2\pi R_{vv}}} \times \exp\Big\{-\frac{1}{2R_{vv}}\Big(p(r_s, z_s, z_\ell) - c\Big[\mathbf{\Phi}_i(z_\ell;\Theta)\Big]\Big)^2\Big\}. \tag{36}$$

Thus, we estimate the posterior distribution using a sequential Monte Carlo approach and construct a *bootstrap particle filter* using the following steps [30]:

- Initialize: $\mathbf{\Phi}_i(0), \mathbf{w}_i \sim \mathcal{N}(0, \mathbf{R}_{ww}), W_i(0) = 1/N_p; i = 1,\cdots,N_p$;
- State Transition: $\mathbf{\Phi}_i(z_\ell;\Theta) = \mathbf{A}(z_{\ell-1})\mathbf{\Phi}_i(z_{\ell-1}) + \mathbf{w}_i(z_{\ell-1})$
- Likelihood Probability: $\Pr[p(r_s, z_s, z_\ell)|\mathbf{\Phi}_i(z_\ell)]$ of Eq. 36;
- Weights: $W_i(z_\ell;\mathbf{\Theta}) = W_i(z_{\ell-1};\mathbf{\Theta}) \times \Pr[p(r_s, z_s, z_\ell)|\mathbf{\Phi}_i(z_\ell)]$;
- Normalize: $\mathcal{W}_i(z_\ell;\mathbf{\Theta}) = \frac{W_i(z_\ell;\mathbf{\Theta})}{\sum_{i=1}^{N_p} W_i(z_\ell;\mathbf{\Theta})}$;
- Resample: $\tilde{\mathbf{\Phi}}_i(z_\ell;\mathbf{\Theta}) \Rightarrow \mathbf{\Phi}_i(z_\ell;\mathbf{\Theta})$;
- Posterior: $\hat{\Pr}[\mathbf{\Phi}(z_\ell;\mathbf{\Theta})|P_\ell] = \sum_{i=1}^{N_p} \mathcal{W}_i(z_\ell:\mathbf{\Theta}) \times \delta\left(\mathbf{\Phi}(z_\ell;\mathbf{\Theta}) - \mathbf{\Phi}_i(z_\ell;\mathbf{\Theta})\right)$; and
- *MAP* Estimate: $\hat{\mathbf{\Phi}}_i(z_\ell;\mathbf{\Theta})_{MAP} = \max_i \ \hat{\Pr}[\mathbf{\Phi}_i(z_\ell;\mathbf{\Theta})|P_\ell]$;
- *CM* Estimate: $\hat{\mathbf{\Phi}}_i(z_\ell;\mathbf{\Theta})_{CM} = \frac{1}{N_p}\sum_{i=1}^{N_p} \mathcal{W}_i(z_\ell;\mathbf{\Theta}) \times \mathbf{\Phi}_i(z_\ell;\mathbf{\Theta})$.

A detailed flow diagram of the particle filter (bootstrap) algorithm is shown in Fig. 3 illustrating the prediction and update steps along with a resampling algorithm to provide convergence. Again more details can be found in the referenced textbooks and papers [30],

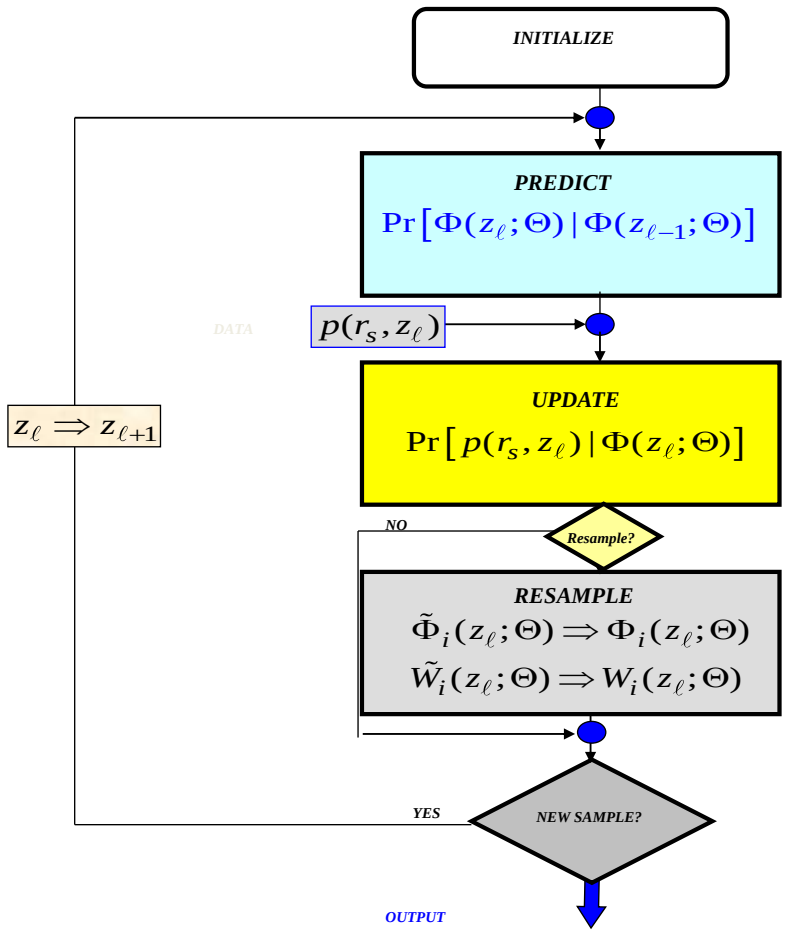

Figure 3: Bootstrap particle filter algorithm flow diagram: prediction, update, and resampling.

4 NELDER-MEADE OPTIMIZER

Many techniques have been developed to perform source localization based on the pressure-field representation which is essentially a product of the modal coefficients and current modal function [6]. We choose to base our localization on a nonlinear least-squares cost function that only incorporates the extracted set of modal coefficients available from the parametrically adaptive processor. These coefficients inherently isolate source location information providing another feature of the parametrically adaptive approach, since it has extracted $\hat{\Theta}$ as part of the state estimation process. Here the *PF* provides estimates of the modal functions $\left\{\hat{\phi}_m(z_\ell)\right\}; \ell = 1, \cdots, L$ over the array, the set of modal coefficients $\left\{\hat{\theta}_m(z_\ell)\right\}; m = 1, \cdots, M$ and the enhanced pressure-field $\left\{\hat{p}(\hat{r}_s, \hat{z}_s; z_\ell)\right\}; \ell = 1, \cdots, L$. With these estimates available, we can solve a nonlinear optimization problem. In fact, rather than using the enhanced pressure-filed exclusively as many of the previous works [3], we use the estimates of the *PF* to provide the set of estimated modal coefficients to the numerical optimizer and take advantage of the state-space model to propagate the modal functions throughout the corresponding "search space". This approach can offer a distinct advantage over simple interpolation schemes, since the *likelihood principle* enables the proposed *MAP* estimates now available at each iteration of the optimizer potentially providing more reliable estimates and a more rapid convergence.

The localization problem solution evolves from the measurement equation of the "depth only" Gauss-Markov model where we can write the sampled pressure-field in terms of range-depth dependent terms as and evolve from the measurement model as

$$p(r_s, z_s, z_\ell) = C'(r_s, z_s)\mathbf{\Phi}(z_\ell) + v(z_\ell) = \underbrace{[\theta_1(r_s, z_s) \;\; 0 \mid \;\; \cdots \;\; \mid \theta_M(r_s, z_s) \;\; 0]}_{C'} \underbrace{\begin{bmatrix} \phi_{11}(z_\ell) \\ \phi_{12}(z_\ell) \\ --- \\ \vdots \\ --- \\ \phi_{M1}(z_\ell) \\ \phi_{M2}(z_\ell) \end{bmatrix}}_{\mathbf{\Phi}} + v(z_\ell) \tag{37}$$

or more compactly

$$p(r_s, z_s, z_\ell) = \sum_{m=1}^{M} \Theta_m(r_s, z_s)\phi_{m1}(z_\ell) + \mathbf{v}(z_\ell); \qquad \ell = 1, \cdots, L. \tag{38}$$

and

$$\theta_m(r_s, z_s) = q \; H_0(k_r(m)r_s)\phi_m(z_s), \tag{39}$$

is the scaled modal coefficient, an implicit, separable function of r_s and z_s. The random noise vectors $\mathbf{w}_\phi$ and $\mathbf{v}$ are assumed Gaussian, zero-mean with respective covariance matrices, $R_{w_\phi w_\phi}$ and R_{vv}. With these definitions in mind it is now possible to define (simply) the *model-based localization problem* as:

GIVEN a set of estimated modal coefficients $\{\hat{\Theta}_m(z_\ell)\}; m = 1, \cdots, M$ (from the *PF*) extracted from noisy pressure-field and sound speed measurements, $[\{p(r_s, z_s, z_\ell)\}, \{c(z_\ell)\}]$, FIND the "best" estimate of the source position (r_s, z_s), that is, FIND $\hat{r}_s$ and $\hat{z}_s$.

In order to solve this problem we must first estimate the "unknown" modal coefficients $\hat{\theta}_m(r_s, z_s)$ from the noisy pressure-field measurement model and then use numerical optimization techniques to perform the localization (r_s, z_s). In the design of a localizer we choose a nonlinear least squares approach.[34] Thus, the optimization problem is to find the source position (r_s, z_s) that minimizes the sum-squared error

$$J(\hat{r}_s, \hat{z}_s) := \frac{1}{M} \sum_{m=1}^{M} \underbrace{\left(\overbrace{\hat{\theta}_m(r_s, z_s)}^{\text{PF}} - \overbrace{H_0\left(\kappa_r(m)\hat{r}_s\right) \phi_m(\hat{z}_s)}^{\text{N-M OPTIMIZER}} \right)}_{\varepsilon}^2 \tag{40}$$

Since we know from our analysis [6] that a unique optimum does exist, we choose to use a brute force, *direct search* method for our localizer primarily because it requires the minimal amount of *a-priori* information and should slowly converge to the global optimum. For an on-line application, more rapidly convergent algorithms requiring a-priori information (gradient and Hessian) should be investigated, [34] but here we use an off-line search to investigate the feasibility of the model-based localization and mention some of these alternatives in the discussion.

The "direct search" localization algorithm follows the *polytope* method of Nelder-Meade (N-M) [34]-[35]. At each stage of iteration, $N + 1$ points, say $\alpha_1, \cdots, \alpha_{N+1}$, are retained together with the function of these values, that is,

$$\alpha_n := (r_n, z_n) \qquad J(\alpha_n) \quad for \quad n = 1, 2, \cdots, N + 1 \tag{41}$$

where the functions are ordered such that

$$J(\alpha_{N+1}) \geq J(\alpha_N) \geq \cdots \geq J(\alpha_1) \tag{42}$$

and constitute the vertices of the polytope in $N-$space. At each iteration, a new polytope is generated producing a new point to replace the "worst" point α_{N+1}—the point with the

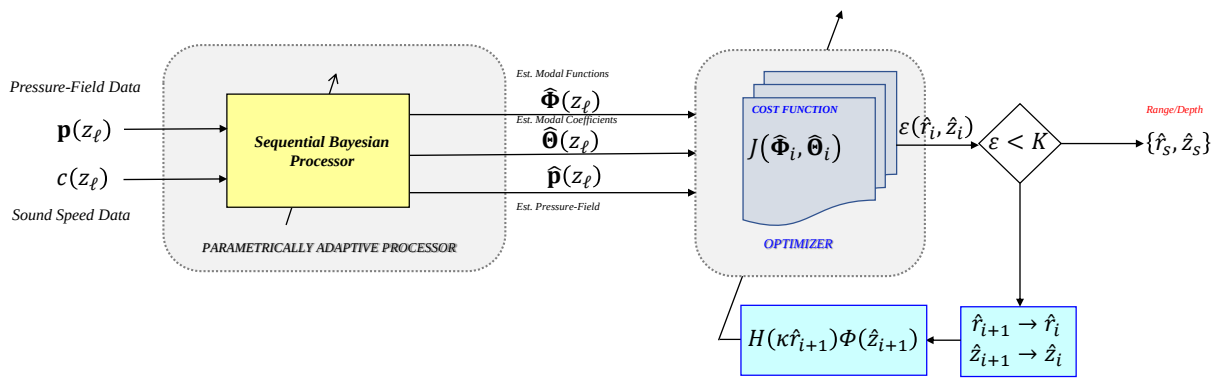

Figure 4: Model-Based Localization: Sequential Processor and Optimizer.

largest function value. If we define $c(\alpha)$ as the centroid of the "best" N vertices $\alpha_1, \cdots, \alpha_N$ given by

$$c(\alpha) = \frac{1}{N} \sum_{n=1}^{N} \alpha_n \tag{43}$$

then at the beginning of the nth-iteration a search or trial point is constructed by a single *reflection* step using

$$\alpha_r = c(\alpha) + (c(\alpha) - \alpha_{N+1})\, \Delta_r \tag{44}$$

where Δ_r is the reflection coefficient ($\Delta_r > 0$). The function is evaluated at α_r giving $J(\alpha_r)$ and yielding three possibilities:

- $J(\alpha_1) \leq J(\alpha_r) \leq J(\alpha_N)$ and therefore $\alpha_r \longrightarrow \alpha_{N+1}$; or
- $J(\alpha_r) < J(\alpha_1)$ and $\alpha_r \longrightarrow \alpha_1$ a new "best" point, since we are minimizing J. The direction Δ_r is assumed correct and we then *expand* the polytope by defining

$$\alpha_e = c(\alpha) + (\alpha_r - c(\alpha))\, \Delta_e \tag{45}$$

  where Δ_e is the expansion coefficient ($\Delta_e > 1$). If $J(\alpha_e) \leq J(\alpha_r)$, $\alpha_e \longrightarrow \alpha_{N+1}$ otherwise $\alpha_r \longrightarrow \alpha_{N+1}$; or

- $J(\alpha_r) > J(\alpha_N)$, the polytope is too large and we must "contract" it using

$$\alpha_c = \begin{cases} \alpha_1 + (\alpha_{N+1} - \alpha_1)\,\Delta_c & for \quad J(\alpha_r) \geq J(\alpha_{N+1}) \\ \alpha_1 + (\alpha_r - \alpha_1)\,\Delta_c & for \quad J(\alpha_r) < J(\alpha_{N+1}) \end{cases} \tag{46}$$

  where Δ_c is the contraction coefficient. If $J(\alpha_c) < min\{J(\alpha_r), J(\alpha_{N+1})\}$, then $\alpha_c \longrightarrow \alpha_{N+1}$.

Using the MATLAB Optimization Toolbox [36], we will apply the polytope N-M optimization algorithm to measured pressure-field data obtaining a set of modal coefficients$\{\theta_m(r_s, z_s)\}, m = 1, \cdots, M$ representing the shallow water discussed in the next section. We will see that the nonlinear least squares fit of $\hat{\theta}_m$ to θ_m, the mean squared error function and the iteration steps lead to the algorithm convergence. This is a well-posed, implicit optimization problem with an optimum solution available as long as the unknown functions $\{\hat{\theta}_m(r_s, z_s)\}$ can be estimated from the noisy pressure-field measurements. We summarize the steps of this parametrically adaptive approach to target localization in Fig. 5.

Before we discuss the details of the *PF*, let us see how we can utilize the model-based approach to implement our localizer. From the cost function $J(r_s, z_s)$ of Eq. 13, we see that we must have an estimate of the modal coefficient function or perhaps more appropriately range-depth function, $\theta_m(r_s, z_s)$ and this is provided by our *PF*. However, we must also have estimates of the associated Hankel function, $H_0(\kappa_r r_n)$ and the corresponding modal functions evaluated at the current iterate depth, z_n as $\phi_{m1}(z_n)$. The *PF* provides us with estimates of these modal functions $\{\hat{\phi}_{m1}(z_\ell)\}, \quad m = 1, \cdots, M; \quad \ell = 1, \cdots, L$ at each sensor location (in depth). Since the optimizer requires a finer mesh (in depth) than the modal function estimates at each sensor to perform its search, we use the state-space propagator to generate the estimates at a finer depth sampling interval

$$\Delta z_n := \frac{\Delta z_\ell}{p} \qquad p \in \mathbf{I} \tag{47}$$

Thus for a given value of "search" depth z_n, we find the closest available depths from the estimator (array geometry) to bracket the target depth, $z_{\ell-1} < z_n < z_\ell$, and use the lower bound $z_{\ell-1}$ to select the initial condition vector for our propagator. We then propagate the modal function at the finer Δz_n to obtain the desired estimate at $\hat{\phi}_{m1}(z_n)$.

Note that the propagator evolves simply by discretizing the differential equation using first differences

$$\frac{d}{dz}\phi(z) \approx \frac{\phi(z_n) - \phi(z_{n-1})}{\Delta z_n} \tag{48}$$

which leads to the corresponding *state-space propagator* given by

$$\hat{\phi}(z_n) = [\mathbf{I} - \Delta z_n A(z_n)]\,\hat{\phi}(z_{n-1}) \qquad for \quad \hat{\phi}(z_{n-1}) = \phi(z_{\ell-1}) \tag{49}$$

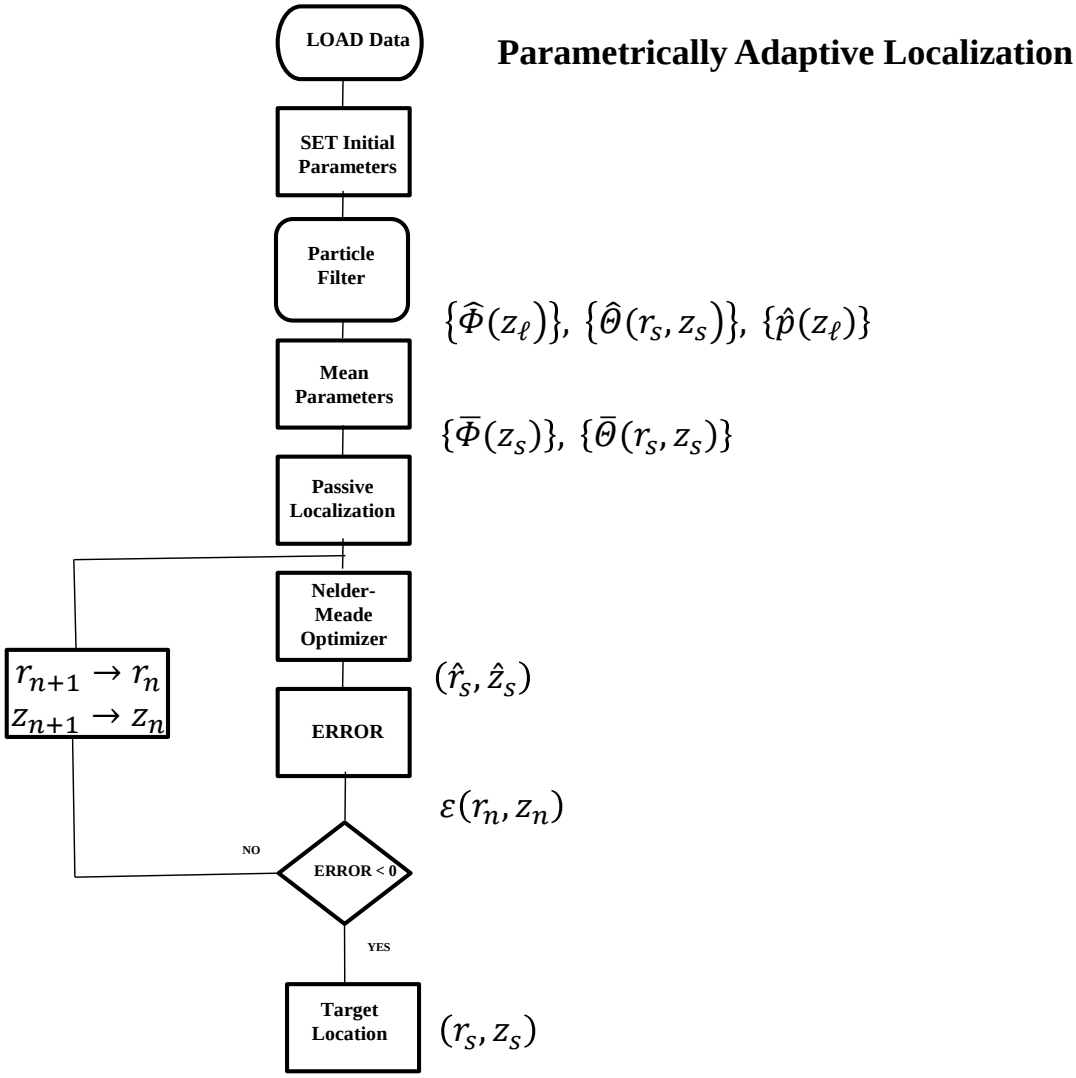

Figure 5: Parametrically Adaptive Localization Algorithm Structure

In this way the state-space propagator is used to provide functional estimates to the nonlinear optimizer for localization, so we see that the *PF* of the next section is designed to not only provide estimates of the range-depth function, but also provide enhanced estimates of the modal functions at each required depth iteration, that is

$$\left[\{\hat{\theta}_m(r_s, z_s)\}, \{\hat{\phi}_{m1}(z_\ell)\}\right] \longrightarrow \left[\{\hat{\phi}_m(z_n)\}, (\hat{r}_s, \hat{z}_s)\right] \tag{50}$$

From an estimation viewpoint, it is important to realize the ramifications of the output of the processor and its relationship to the position estimates. The respective modal coefficient/range-depth and modal function estimates $\hat{\theta}$ and $\hat{\phi}$ provided by the processor are minimum variance estimates (approximately) as illustrated in Fig. 4. In the case of Gaussian noise, they are, if fact, the maximum likelihood (maximum a-posteriori) estimates and therefore the corresponding maximum likelihood *invariance theorem* guarantees that the solutions for the (r_s,z_s) are also the maximum likelihood estimates of position [4].

This completes the description of the model-based localizer, next we discuss how the modal functions and their corresponding coefficients are estimated from noisy pressure-field measurements by developing the *PF*.

5 LOCALIZATION: HUDSON CANYON EXPERIMENT

In this section we discuss the development of the model-based localizer for the Hudson Canyon experiment performed in 1988 in the Atlantic with the primary goal of investigating acoustic propagation (transmission and attenuation) using continuous wave data [23], [24]. The Hudson Canyon is located off the coast of New Jersey in the area of the Atlantic Margin Coring project borehole 6010 . The seismic and coring data are combined with sediment properties measured at that site. Excellent agreement was determined between the model and data indicating a well-known, well-documented shallow water experiment with bottom interaction and yielding ideal data sets for investigating the applicability of a processor to measured ocean acoustic data. The experiment was performed at low frequencies ($50 - 600Hz$) in shallow water of $73m$ depth during a period of calm sea state as shown in Fig. 6. A calibrated acoustic source was towed at roughly $36m$ depth along the $73m$ isobath radially to distances of 4 to $26Km$. The ship speed was between 2 and $4Kts$. The fixed vertical hydrophone array consisted of 24 phones spaced $2.5m$ apart extending from the seafloor up to a depth of about $14m$ below the surface. The current-temperature-density (*CTD*), sound-speed profiles (*SSP*), measurements were made at regular intervals and the data were collected under carefully controlled conditions in the ocean environment. The normalized horizontal wavenumber spectrum for a $50Hz$ temporal frequency is dominated by 5 modes occurring at wavenumbers between 0.14 to $0.21m^{-1}$ with relative amplitudes increasing at increased wavenumbers. A SNAP [26] simulation was performed and the results agree quite closely, indicating a well-understood ocean environment.

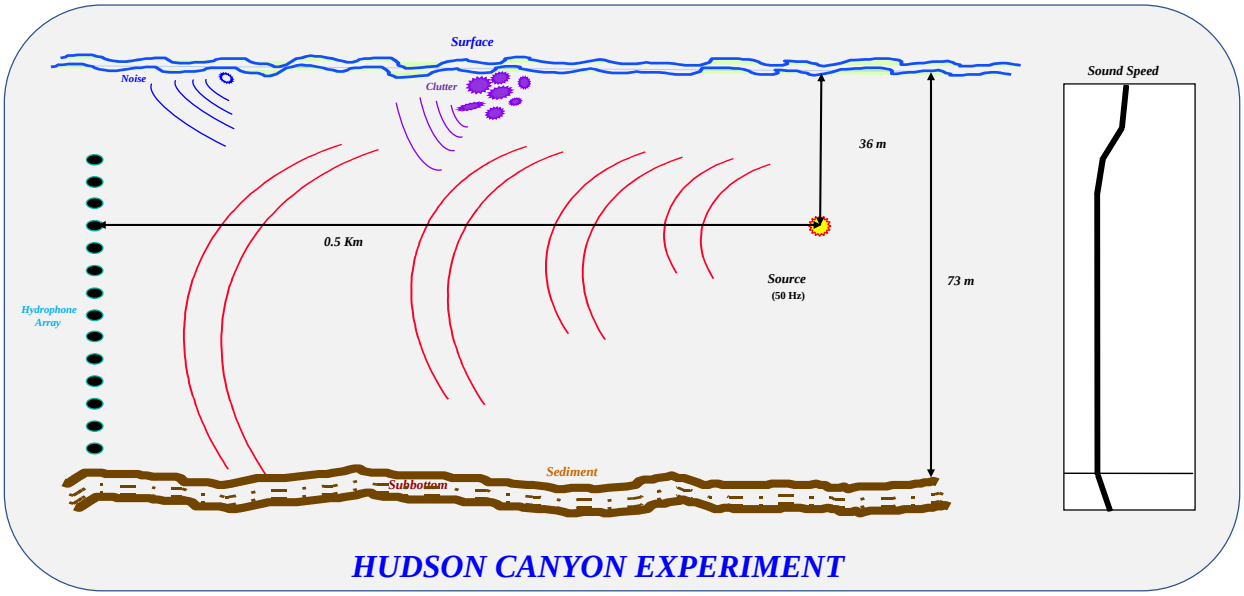

Figure 6: Hudson Canyon experiment geometry and structure: (a) Source at 36m depth and 0.5 Km range, 50 Hz. (b) 23-element vertical hydrophone array. (c) 5-modes support the water column.

In order to construct the state-space localizer (see Fig. 2), we require the set of parameters which were obtained from the experimental measurements and processing. The horizontal wavenumber spectra were estimated using synthetic aperture processing [23]. Eight temporal frequencies were employed: four on the inbounds $(75Hz, 275Hz, 575Hz, 600Hz)$ and four on the outbound $(50Hz, 175Hz, 375Hz, 425Hz)$. In this application we will confine our investigation to the $50Hz$ case, which is well-documented, and to horizontal ranges from $0.5 - 4Km$. The raw measured data was processed (sampled, corrected, filtered, etc.) and supplied for this investigation.

5.1 Particle Filter Design and Analysis

The design and development of the parametrically adaptive *PF* proceeds through the following steps: (1) pre-processing the raw experimental data; (2) solving the boundary value problem (*BVP*) [26] to obtain initial parameter sets for each temporal frequency (e.g. modal coefficients, wavenumbers, initial conditions, etc.); (3) state-space forward propagator simulation of synthetic data for *PF* analysis/design; (4) application to measured data; and (5) *PF* performance analysis as shown in Fig. 2.

Pre-processing of the measured pressure-field data follows the usual pattern of filtering,

outlier removal and Fourier transforming to obtain the complex pressure-field as a function of depth along the array. This data along with experimental conditions (frequencies, *CTD SSP* boundary conditions, horizontal wavenumber estimators (see [7] for details) provide the input to the normal mode *BVP* solutions (SNAP [27], KRACKEN [28], SAFARI [29]) yielding the output parameters. These parameters are then used as input to the state-space forward propagator (see Fig. 2) developed in Sec. 2.

After obtaining a reasonable representation of the 50 Hz Hudson Canyon data, the particle filter consisting of $10K$-particles was developed and applied to the noisy pressure-field measurements. A 100-member ensemble of *PF* runs were collected, each representing a unique realization of the solution. Both the "average" maximum-a-posteriori (*MAP*) and conditional mean (*CM*) estimates for the modal functions and coefficients as well as the pressure-field measurements are shown in Figs. 7-9 providing a reasonable perspective of the parametrically adaptive *PF* performance. In Fig. 7 we see the estimated, ensemble averaged, modal functions ($\hat{\Phi}(z_\ell;\Theta)$) with reasonable estimates of the last 3 functions; however, those of the first and second functions appear to be biased. These estimates will clearly affect the accuracy of the localizer. The "average" modal coefficient parameter estimates are shown in Fig. 8 where we observe instantaneous estimates of each at depth. The bias appearing in the first modal estimate is now obvious from its corresponding coefficient estimate compared to the true fixed mean value explaining the bias. The estimated pressure-field appears to be quite reasonable for both the *MAP* and *CM* ensemble estimates with the exception of the invalid start-up guesses. Classical metrics such as innovations zero-mean/whiteness testing and weighted sum-squared residual test pass their bounds indicating a reasonable performance of the particle filter. In fact, the pressure-field posterior distributions predicted by the *PF* appear to be unimodal along the array indicating a good likelihood representation. A glimpse of the modal function, Gaussian-like, set of posterior distributions for modal functions 2 and 5 are shown in Fig. 9 (a) and (b) as well modal coefficient estimates of 2 and 3—all representing multi-modal posteriors indicating the correct choice of a *PF* for solution. We also illustrate the multi-modal aspect of the oceanic data by observing the modal function posterior *PDF* estimates for modes 1 and 5 in Fig. 10. It is clear from the plots that for each depth, multiple peaks appear in the posterior estimates. The pressure-field posterior is better behaved almost producing a near unimodal posterior for the predicted field. Visualizing a peak at each depth produces a "smooth" estimate (*MAP*) as shown in Fig. 11. This completes the analysis of the Hudson Canyon experimental data and the adaptive (modal coefficient) *PF* processing performance.

A more thorough investigation of these distributions at various depth (slices: $2, 3, 6, 11$ m) clearly substantiate this choice of processor as shown in Fig. 12. Another metric to validate the performance of the processor is the Hellinger distance that compares the "true" posterior distribution predicted by the model to that estimated distribution produced by the *PF* from the measured data for both modal functions and coefficients. Again the results (Hellinger [30] close to zero) indicates a reasonable *PF* design as observed by the posterior distributions in Fig. 13. This completes the design and analysis of the particle filter for this

shallow ocean application. These results can be compared to those obtained in Refr. [7] before on similar data from the Hudson Canyon.

For a given realization, the modal coefficient estimates and relative error statistics comparing them to the mean values are shown in Table 1. Calculating the average relative error from these estimates we see that they appear quite good (for this realization) with both the *CM* (0.95%) and *MAP* (0.88%) estimates less than 1%. Over the 100-member ensemble the *MAP* estimates yield approximately an average relative error of 2.5%—again quite reasonable for this application.

Table I. Model-Based Identification: *PF* Modal Coefficient Estimation

Modal Coeff.	Mean	CM	$\epsilon_{CM}(\%)$	MAP	$\epsilon_{MAP}(\%)$	$\overline{MAP}$	$\bar{\epsilon}_{MAP}(\%)$
θ_1	1.000	1.002	0.281	1.003	0.330	0.983	1.675
θ_2	0.673	0.677	0.633	0.675	0.327	0.665	1.192
θ_3	0.163	0.165	1.374	0.164	0.246	0.161	1.553
θ_4	0.166	0.167	0.661	0.169	1.651	0.165	0.809
θ_5	0.115	0.117	1.816	0.117	1.757	0.118	7.487
AVG $\epsilon(\%)$			0.953		0.882		2.54

This completes the analysis of the performance of the adaptive particle filter for the modal coefficient estimates. It is clear from these ensemble runs that the *PF* is capable of parametrically adapting to the changing shallow ocean environment in both these cases providing reasonable tracking estimates of the modal functions while simultaneously estimating the associated pressure-field and unknown parameters.

5.2 Model-Based Localization

With the *PF* design available, the development of the model-based localizer follows. Recall that the cost function is based on the comparison of the estimated modal coefficients from the *PF* to that calculated from the scaled, range (Hankel) and depth (state transition) functions at the various search locations $(\hat{r}_s, \hat{z}_s)$, that is,

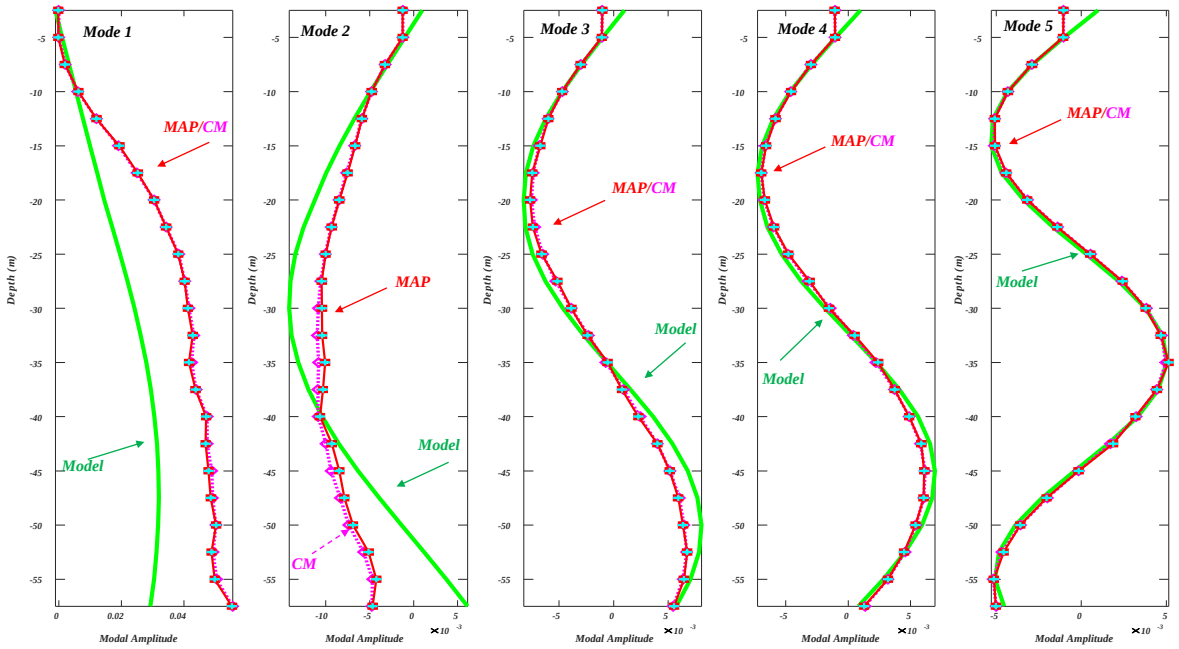

Figure 7: Sequential Bayesian Processor (100-Member Ensemble): Modal Function Estimation.

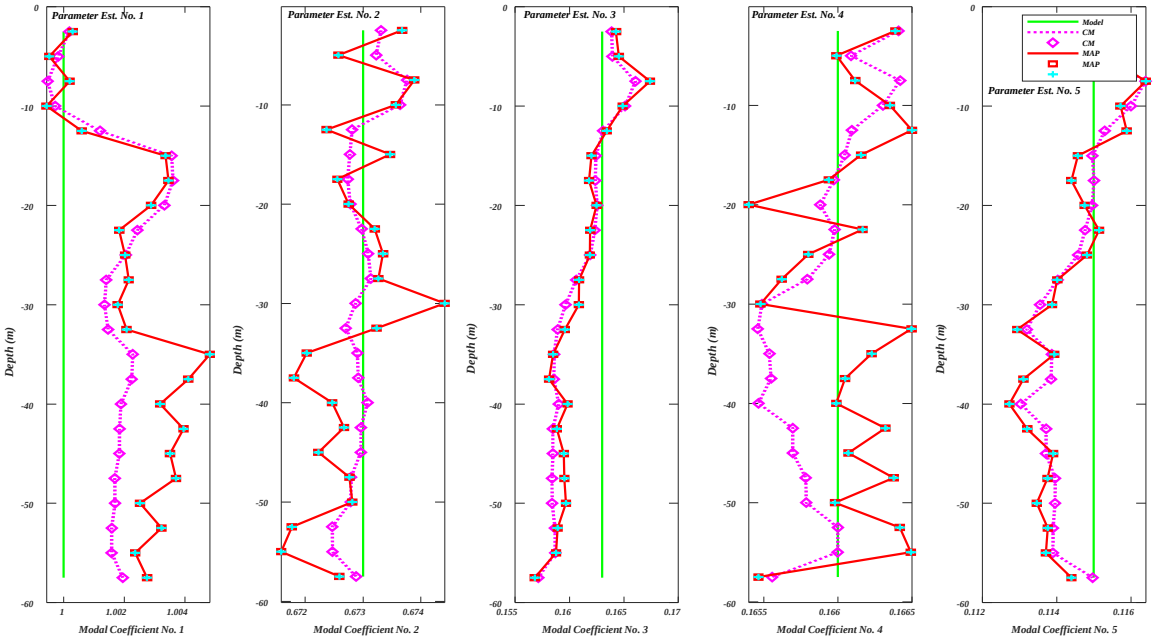

Figure 8: Sequential Bayesian Processor (100-Member Ensemble): Modal Coefficient Estimation.

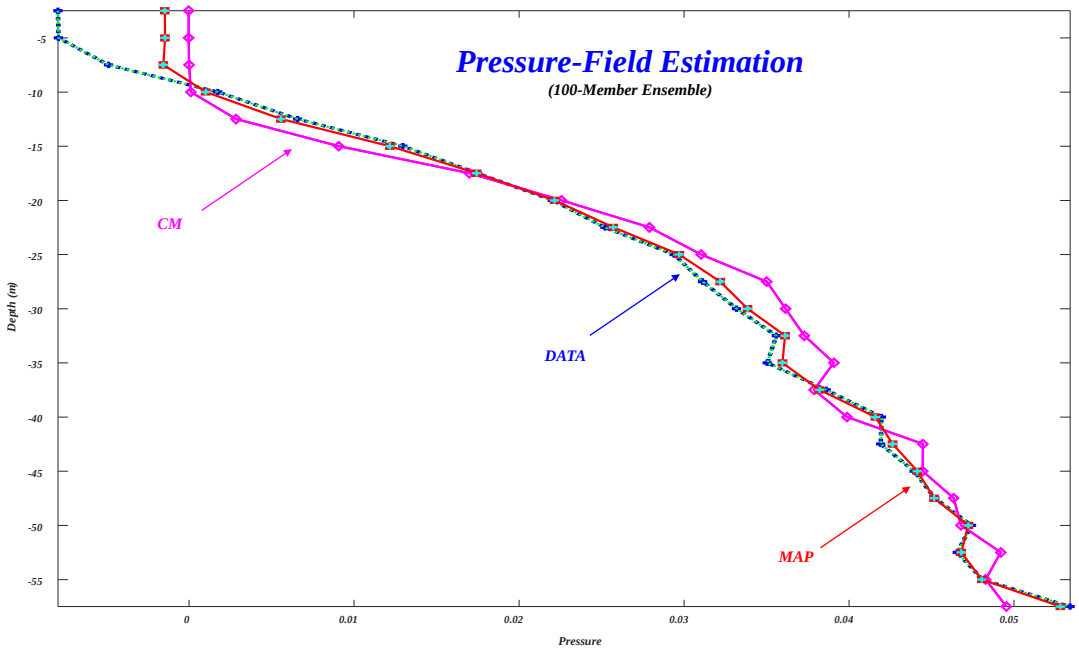

Figure 9: Sequential Bayesian Processor (100-Member Ensemble): Pressure-Field Estimation.

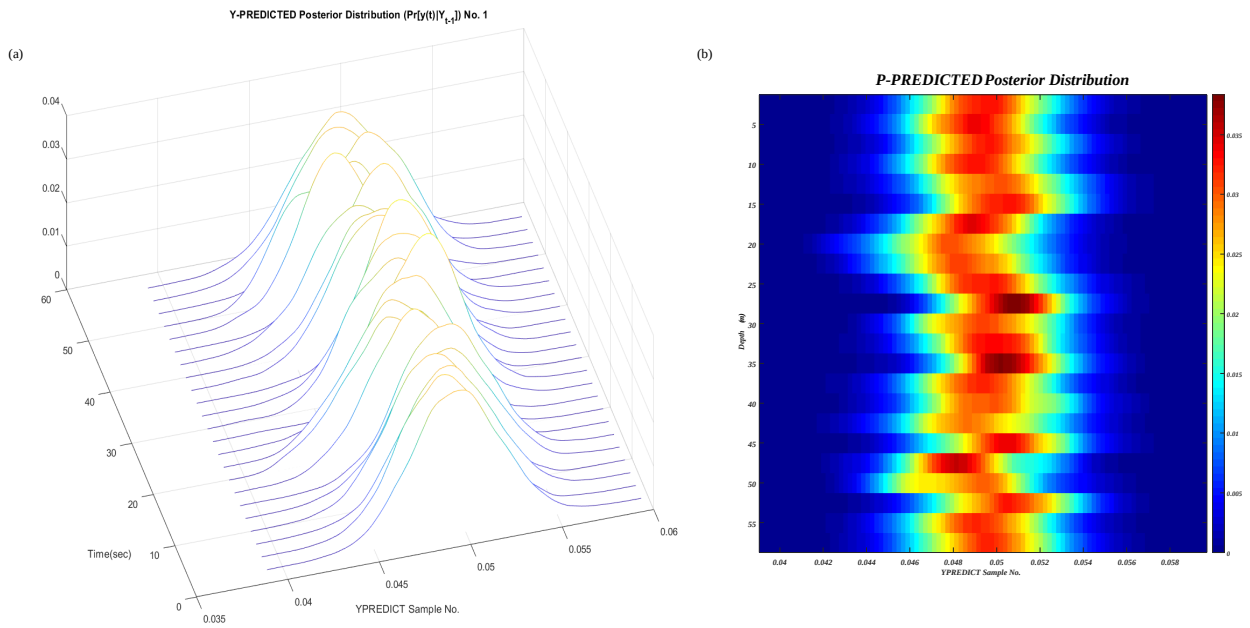

Figure 10: Sequential Bayesian Processor (100-Member Ensemble): Estimated Pressure-Field Distribution.

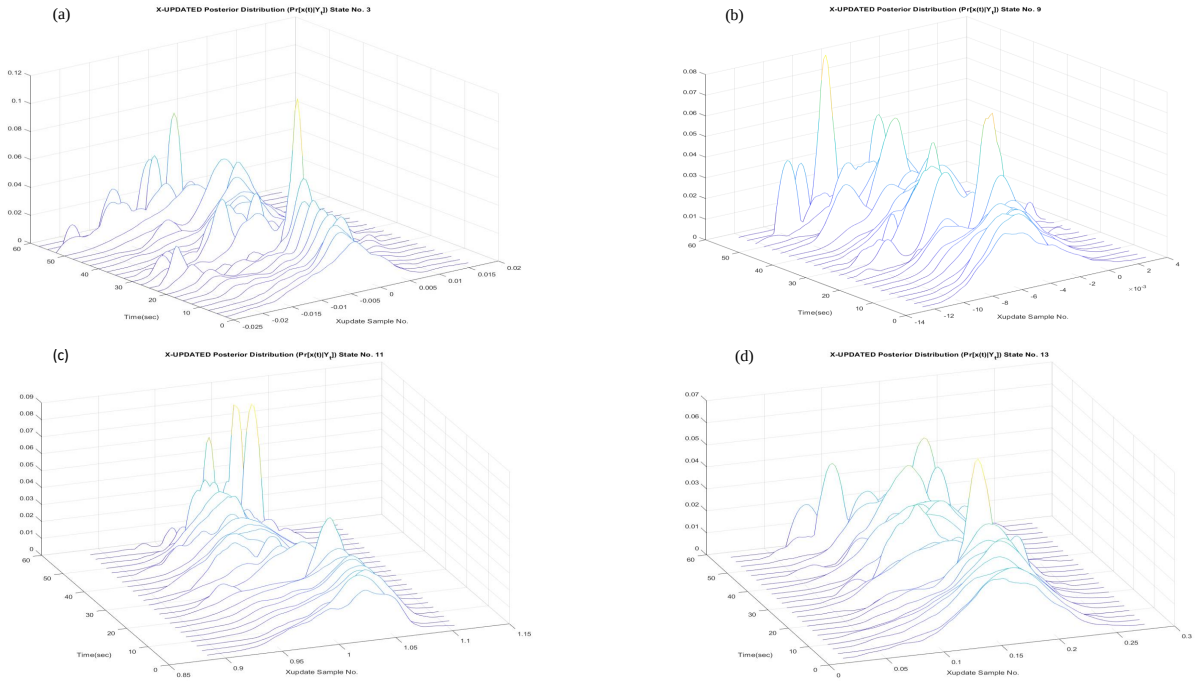

Figure 11: Sequential Bayesian Processor (100-Member Ensemble): Estimated Modal Distributions for No. 2/5 (a)/(b) and Modal Coefficient Distributions 2/3 (c)/(d).

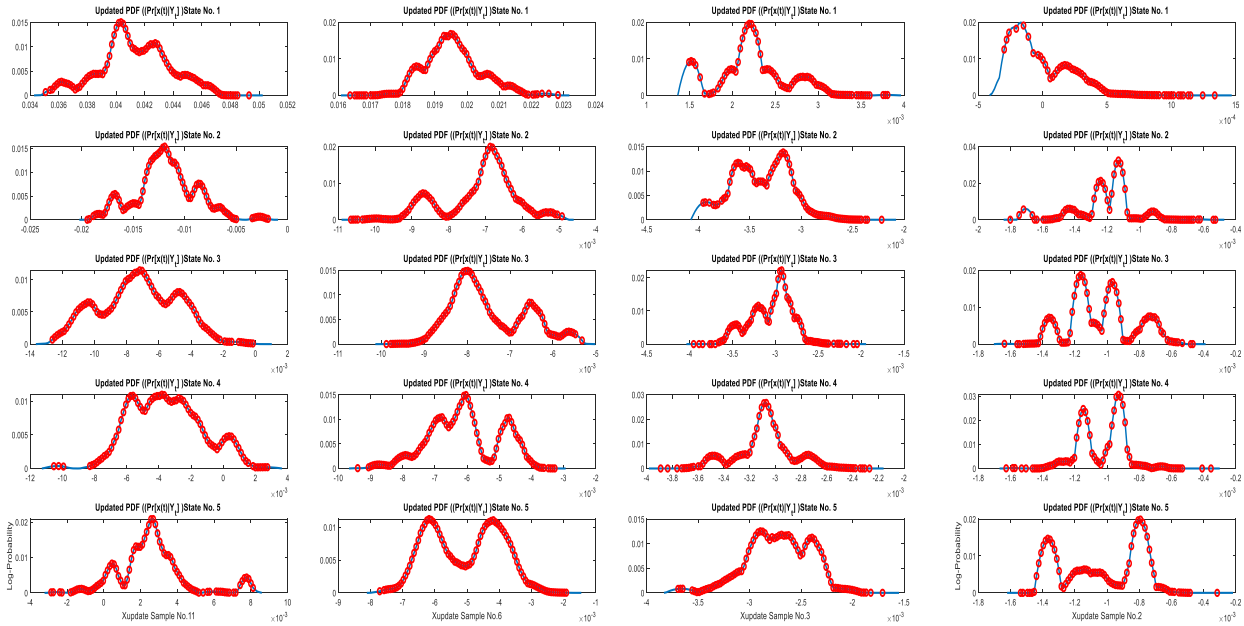

Figure 12: Sequential Bayesian Processor (100-Member Ensemble): Estimated Modal Distributions (Depth Slices) at $11, 6, 2, 3$ meters.

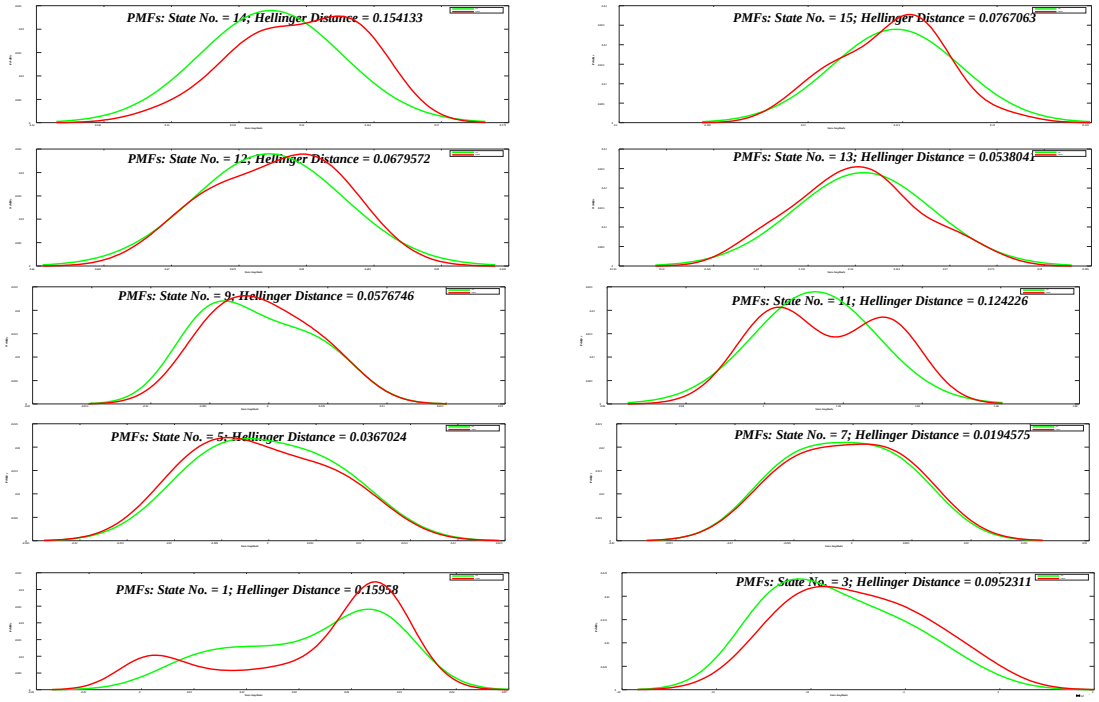

Figure 13: Sequential Bayesian Processor (100-Member Ensemble): Hellinger Distributions for Mode Estimates $(1-5)$ and Modal Coefficients $(1-5)$.

$$J(\hat{r}_s, \hat{z}_s) := \frac{1}{M} \sum_{m=1}^{M} \underbrace{\left(\overbrace{\hat{\theta}_m(r_s, z_s)}^{\text{PF}} - \overbrace{H_0\left(\kappa_r(m)\hat{r}_s\right)\phi_m(\hat{z}_s)}^{\text{N-M OPTIMIZER}} \right)}_{\varepsilon}^2 \tag{51}$$

Executing the model-based localizer over the Hudson Canyon pressure-field data yields the following results for a typical data set. In Fig. 14(a) we see the modal coefficient estimates compared to the true (mean values), mean (sum) squared errors and the search values $(\hat{r}_s, \hat{z}_s)$ at each iteration produced by the N-M optimizer. The true (mean) source depth was measured at $(500m, 36m)$ while the model-based localizer estimates were $(495m, 35m)$—quite reasonable for a 5.2% relative error initial guess of $(475m, 34.2m)$. In Fig. 14(b) we show the results of the optimizer search over the range/depth space. Each step is shown for a 100-step limit producing the above results. It is also interesting to observe the final modal coefficient estimates obtained from the median estimates across the array for each parameter. For this realization, it appears the 3rd coefficient has the largest error. We chose the median rather than the average to account for outliers that might have resulted during the estimation providing a more robust modal coefficient estimate.

As a final test of this approach, we generated an ensemble of 100-localization trials with the average performance for range and depth estimates resulting in:

$$\begin{aligned} \text{Range} &= 495.34 \text{ meters} - - - (\overline{\epsilon}_{REL} \;=\; 0.93\%) \\ \text{Depth} &= 38.2 \text{ meters} - - - (\overline{\epsilon}_{REL} \;=\; 6.1\%) \end{aligned}$$

with the accompanying relative errors. These results are quite reasonable for the target localization in a noisy shallow ocean environment.

6 SUMMARY

In this report we have developed a model-based sequential Bayesian solution to the ocean acoustic localization problem based on the normal-mode propagation model and a vertical sensor array measurement system. We demonstrated that a parametrically adaptive particle filter is capable of estimating the modal functions while jointly extracting modal coefficients in an ever changing shallow ocean environment. These estimates were provided as input to a numerical (simplex) optimizer and incorporated into a model-based localization scheme.

Over the 100-member ensemble the *MAP* estimates yield approximately an average relative error of 2.5% with the corresponding localizer (optimizer) producing relative range/depth errors of 0.93% and 6.1%, respectively—again quite reasonable for this application. Thus,

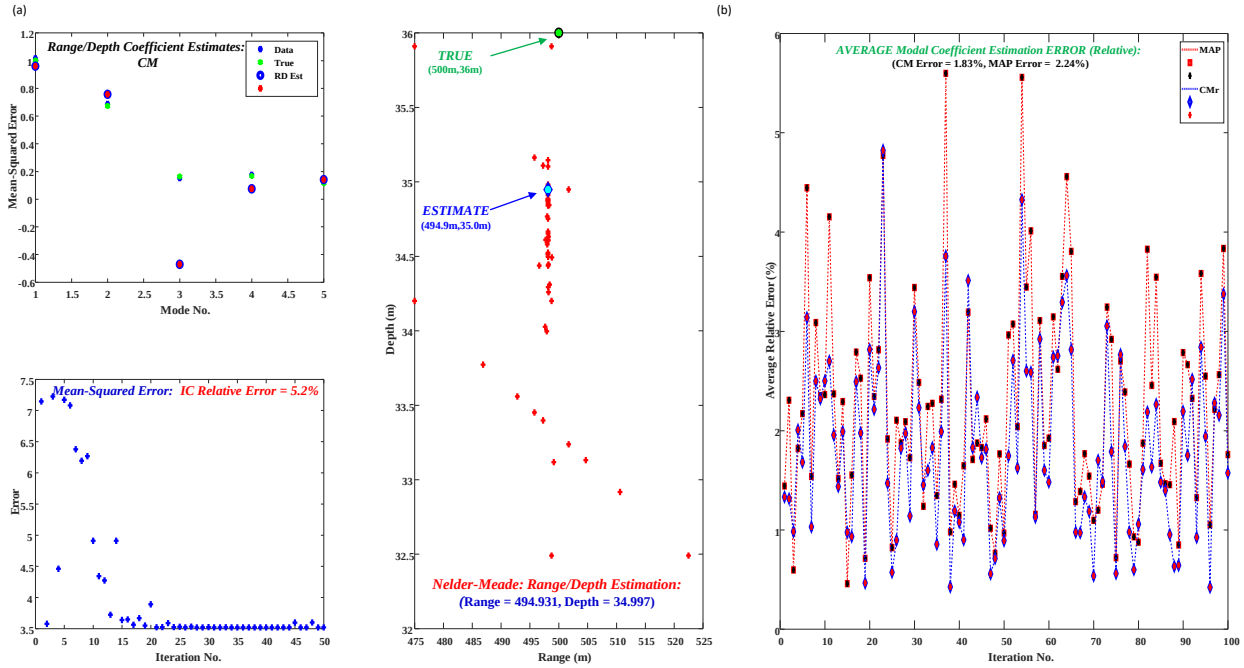

Figure 14: Model-Based CM Localizer (5.2% Relative IC Error): (a) Range/Depth Estimation (single realization): Range/Depth Parameter estimation, mean-squared error, optimization (Range: 494.9m,Depth 35.0m). (b) Average CM (1.84%) and MAP (2.24%) relative estimation errors .

the performance of the *PF* over a 100-member ensemble to evaluate its performance and the localizer was shown to produce a reasonable estimation of the target location.

ACKNOWLEDGMENTS

This work performed under the auspices of the U.S. Department of Energy by Lawrence Livermore National Laboratory under Contract DE-AC52-07NA27344.

References

[1] C. S. Clay, and H. Medwin, *Acoustical Oceanography.* New York:Wiley, 1977, 544 pp.

[2] C. S. Clay, "Use of arrays for acoustic transmission in a noisy ocean," *Res. Geophys.*, **4**, (4), 475-507, 1966.

[3] C. Yardim, Z-H. Michalopoulou and P. Gerstoft, "An overview of sequential Bayesian filtering in ocean acoustics", *IEEE J. Oceanic Eng.*, **36**, (1), 73-91, 2011.

[4] M. J. Hinich, "Maximum likelihood signal processing for a vertical array," *J. Acoust. Soc. Am.*, **54**, 499-503, 1973.

[5] J. V. Candy and E. J. Sullivan. "Ocean acoustic signal processing: a model-based approach." *J. Acoust. Soc. Am.*, **92**, (12), 3185-3201, 1992.

[6] J. V. Candy, and E.J. Sullivan, "Passive localization in ocean acoustics: a model-based approach," *J. Acoust. Soc. Am.*, **98**, (3), 1455-1471, 1995.

[7] J. V. Candy, "Environmentally adaptive processing for shallow ocean applications: A sequential Bayesian approach," *J. Acoust. Soc. Am.*, **138**, (3), 1268-1281, 2015.

[8] H .P. Bucker, "Use of calculated sound fields and matched-field detection to locate sound in shallow water," *J. Acoust. Soc. Am.*, **59**, 329-337, 1976.

[9] A. B. Baggeroer, W. A. Kuperman, and H. Schmidt, "Matched-field processing: source localization in correlated noise as an optimum parameter estimation problem," *J. Acoust. Soc. Am*, **83**, (2), 571-587, 1988.

[10] E.C. Shang, C.S. Clay and Y.Y. Wang, "Passive harmonic source ranging in wavguides by mode filtering." *J. Acoust. Soc. Am.*, **78**, (1), 172-175, 1985.

[11] T.C. Yang, "A method of range and depth estimation by modal decomposition." *J. Acoust. Soc. Am.*, **82**, (5), 1736-1745, 1987.

[12] G. Wilson, R. Koch and P. Vidmar, "Matched mode localization." *J. Acoust. Soc. Am.*, **84**, (1), 310-320, 1988.

[13] E.C. Shang, "An efficient high resolution method of source localization processing in mode space." *J. Acoust. Soc. Am.*, **86**, (5), 1960-1964, 1989.

[14] T.C. Yang, "Effectiveness of mode filtering: a comparision of matched-field and matched-mode processing." *J. Acoust. Soc. Am.*, **87**, (5), 2072-2084, 1989.

[15] E. J. Sullivan and D. Middleton, "Estimation and detection issues in matched-field processing", *IEEE J. Oceanic Eng.*, **18**, (3), 156-167, 1993.

[16] C. Feuillade, D. Del Balzo, and M. Rowe, "Environmental mismatch in shallow-water matched-field processing: geoacoustic

[17] A. Tolstoy. *Matched Field Processing for Ocean Acoustics*. New Jersey:World Scientific Publishing Co., 1993.

[18] R. D. Doolittle, A. Tolstoy and E.J. Sullivan, ' "Special Issue on Detection and estimation in matched-field processing" *IEEE Trans. Ocean Eng.*, **18**, (3), 1993.

[19] A. M. Richardson, and L. W. Note, "A posteriori probability source localization in an uncertain sound speed, deep ocean environment," *J. Acoust. Soc. Am.*, **89**, (6), 2280-2284, 1991.

[20] W. A. Kuperman, M.D. Collins, J.S. Perkins and N.R. Davis "Optimum time domain beamforming with simulated annealing including application of a-priori information," *J. Acoust. Soc. Am.*, **88**, 1802-1810, 1990.

[21] E. J. Sullivan, *Model-Based Array Signal Processing*, New York: Springer, 2015.

[22] J. L. Krolik, "Matched-field minimum variance beamforming in a random ocean channel," *J. Acoust. Soc. Am.*, **92**, (3), 1408-1419, 1992.

[23] W. M. Carey, J. Doutt, R. Evans and L. Dillman, "Shallow water transmission measurements taken on the New Jersey continental shelf," *IEEE J. Oceanic Eng.*, **20**, (4), 321-336, 1995.

[24] A. R. Rogers, Y. Yamamoto and W. Carey, "Experimental investigation of sediment effect on acoustic wave propagation in shallow water," *J. Acoust. Soc. Am.*, **93**,1747-1761, 1993.

[25] J. V. Candy, *Model-Based Signal Processing*. Hoboken, N.J.:Wiley/IEEE Press, 2006, 677 pp.

[26] F. B. Jensen, Kuperman, W. A., Porter M. B.,and H. Schmidt, *Computational Ocean Acoustics* New York: Amer. Instit. Physics Press, 1994, 455 pp.

[27] F. B. Jensen and M. C. Ferla, "SNAP: the SACLANTCEN normal-model propagation model," *Report SM-121*, Italy: SACLANTCEN, 1979, 177 pp.

[28] M. B. Porter, "The KRACKEN normal mode program," *Report SM-245*, Italy: SACLANTCEN, 1991, 183 pp.

[29] H. Schmidt, "SAFARI: Seismo-acoustic fast field algorithm for range independent environments," *Report SM-245*, Italy: SACLANTCEN, 1987, 142 pp.

[30] J. V. Candy, *Bayesian Signal Processing: Classical, Modern and Particle Filtering Methods*. 2^e. Hoboken, N.J.:Wiley/IEEE Press, 2016, 445 pp.

[31] B. Ristic, S. Arulampalam and N. Gordon, *Beyond the Kalman Filter: Particle Filters for Tracking Applications*, Boston: Artech House, 2004, 309 pp.

[32] S. Godsill and P. Djuric, "Special Issue: Monte Carlo methods for statistical signal processing." *IEEE Trans. Signal Proc.*, vol. **50**, 2002 423 pp.

[33] P. Djuric, J. Kotecha, J. Zhang, Y. Huang, T. Ghirmai, M. Bugallo and J. Miguez, "Particle Filtering," *IEEE Signal Proc. Mag.* vol. **20**, No. 5, 19-38, 2003.

[34] P.E. Gill, W. Murray and M.H. Wright, *Practical Optimization*. New York:Academic Press, 1981.

[35] J.A. Nelder and R. Mead, "A simplex method for function minimization", *Computer Journal*, **7**, 308-313, 1965.

[36] A. Grace, *Optimization toolbox for use with MATLAB*, Boston: The MathWorks, 1992.